AIAA JOURNAL
Vol. 46, No. 1, January 2008

Two Error Bounds for Dynamic Condensation Methods

Christophe Lecomte*
University of Cambridge, Cambridge, England CB2 1PZ, United Kingdom
and
J. Gregory McDaniel† and Paul E. Barbone‡
Boston University, Boston, Massachusetts 02215

DOI: 10.2514/1.29866

The dynamic response of large structural systems is often approximated by condensing the systems into smaller subspaces. Among condensation methods, modal condensation and Krylov projection methods have the capability of generating excellent approximations of the response in a selected frequency band. Here are presented error bounds on the response in the band to complement these and other Galerkin Rayleigh–Ritz condensation methods. The bounds guarantee that the magnitude of the error is below the computed threshold. They are based on the expansion of exact expressions of the error using interior and exterior eigenpairs. The interior error is bounded by using existing error bounds on the interior eigenpairs. Sylvester's theorem allows one to determine if all interior eigenvalues are approximated. The exterior error is bounded by using the Cauchy–Schwarz inequality and matrices that bound the restriction of the system matrix to the exterior eigenpairs. Two general algorithms are presented as a general framework to compute bounds on the eigenpairs and bounds on the error and the response. They can be specialized to particular implementations of Rayleigh–Ritz and/or Krylov methods. The application of the bounds is illustrated on a variety of condensation methods and problems.

Nomenclature

$\mathbf{B}_t(\lambda)$	=	matrix based on the extension of $\mathbf{E}_t(\Lambda_E, \lambda)$ to the whole spectrum, for $t = a, b$
$b(\lambda)$	=	bound on the absolute value of the error in the approximation of the transfer function
$\boldsymbol{c}$	=	output vector
E	=	set of indices of Ritz values complementary to the set I
$\mathbf{E}_t(\mathbf{\Lambda}_E, \lambda)$	=	diagonal matrix whose coefficients are $e_t(\lambda_e, \lambda)$, for $t = a, b$
$e(\lambda)$	=	error on the approximation of the transfer function
$e_t(\lambda_e, \lambda)^{-1}$	=	scalar bound on $(\lambda_e - \lambda)^{-1}$, for $t = a, b$
$\boldsymbol{e}_i$	=	ith unit vector such that $\mathbf{I} = \begin{bmatrix} \boldsymbol{e}_1 & \boldsymbol{e}_2 & \dots \end{bmatrix}$
$\boldsymbol{f}$	=	force vector
$g(\lambda)$	=	transfer function
$\tilde{g}(\lambda)$	=	approximation of the transfer function
I	=	set of indices of Ritz values that match actual eigenvalues in the interval of interest
$I_2(f)$	=	integral of the square of the function f in the frequency band, where the transfer function is finite
$I_{2,\text{rel}}(f)$	=	value of the integral $I_2(f)$ relative to the integral $I_2(\tilde{g})$ of the approximate transfer function
$\mathbf{I}$	=	identity matrix
$\mathbf{K}$	=	stiffness matrix
$\mathcal{K}_M[\mathbf{A}, \mathbf{b}]$	=	Krylov subspace defined as the subspace spanned by the vectors $\boldsymbol{b}, \boldsymbol{A}\boldsymbol{b}, \dots, \boldsymbol{A}^{M-1}\boldsymbol{b}$
$\mathbf{M}$	=	mass matrix
M	=	dimension of the reduced model
$\min(S)$	=	minimum of the elements of a set S
$\min_j(f_j)$	=	minimum among all the values f_j indexed by j
N	=	number of degrees of freedom of the original system
N_{miss}	=	deficit of interior Ritz values compared with the number of interior eigenvalues
N_{prec}	=	number of precise interior Ritz values
$\mathbf{r}(\lambda)$	=	residual in forced response problem
$S[\mathbf{E}_t, \mathbf{v}(\lambda)]$	=	bound to correct the extension of $\mathbf{E}_t$ to the whole spectrum, for $t = a, b$, $\mathbf{v}(\lambda) = \mathbf{r}(\lambda), \boldsymbol{c}$
$\mathbf{s}_m$	=	residual in eigenvalue problem
$\mathbf{T}$	=	transformation matrix
$\boldsymbol{x}(\lambda)$	=	forced response vector
$\tilde{\boldsymbol{x}}(\lambda)$	=	approximation of forced response vector
δ	=	tolerance for the confidence intervals
$\delta_{\phi,i}$	=	term in bound on the error on inner products by an approximate eigenvector
$\varepsilon_{\lambda,m}$	=	bound on the error on the approximation of an eigenvalue
$\varepsilon_{\phi,m}$	=	bound on the error on the approximation of an eigenvector
$\boldsymbol{\kappa}$	=	condensed stiffness matrix
$\mathbf{\Lambda}$	=	diagonal matrix of eigenvalues
λ	=	frequency parameter
λ_n	=	nth eigenvalue
$\tilde{\lambda}_n$	=	approximation of the nth eigenvalue (Ritz value)
$\lambda_{\min}, \lambda_{\max}$	=	minimum and maximum of frequency parameter
λ_{band}	=	maximum of frequency parameter in a low-frequency band
$\boldsymbol{\mu}$	=	condensed mass matrix
σ	=	interpolation point
$\mathbf{\Phi}$	=	matrix whose columns are the eigenvectors
$\tilde{\mathbf{\Phi}}$	=	matrix whose columns are the Ritz vectors
$\boldsymbol{\phi}_n$	=	nth eigenvector
$\hat{\boldsymbol{\phi}}_n$	=	nth eigenvector of the reduced system (in the smaller dimension space)
$\tilde{\boldsymbol{\phi}}_n$	=	approximation of the nth eigenvector (Ritz vector)
$\boldsymbol{\psi}_m$	=	arbitrary vector
$\| \mathbf{v} \|$	=	two-norm of a real vector, $\| \mathbf{v} \| = \sqrt{\mathbf{v}^T\mathbf{v}}$

Received 19 January 2007; revision received 1 August 2007; accepted for publication 3 August 2007.

*Research Associate, Department of Engineering.
†Associate Professor, Aerospace and Mechanical Engineering Department. Member AIAA.
‡Associate Professor, Aerospace and Mechanical Engineering Department.

Subscripts

I	=	values associated to the interior set I
i	=	value associated to a particular eigenpair, $i \in I$
E	=	values associated to the exterior set E
e	=	value associated to a particular eigenpair, $e \in E$
m	=	index of a particular Ritz pair
n	=	index of a particular eigenpair
t	=	index of a particular type of bound on the exterior error, $t = a$ or b

I. Introduction

MANY efficient numerical methods have emerged in the past few decades or so to solve approximately the large-scale dynamic system $(\mathbf{K} - \lambda\mathbf{M})\boldsymbol{x}(\lambda) = \boldsymbol{f}$ in a frequency band of interest $\lambda \in [\lambda_{\min}, \lambda_{\max}]$. Among these are Rayleigh–Ritz condensation methods which include Lanczos methods and Krylov projection methods. To assess the quality of these approximations, error bounds on the response of the dynamic system are presented here based on Rayleigh–Ritz condensation methods. One characteristic of these methods, also known as projection or condensation methods, is that one searches for an approximation of the solution $\tilde{\boldsymbol{x}} = \mathbf{T}\mathbf{y}$ in a trial subspace spanned by the columns of $\mathbf{T}$. Usually, the residual $\boldsymbol{f} - (\mathbf{K} - \lambda\mathbf{M})\tilde{\boldsymbol{x}}$ is orthogonal either to the trial subspace (*Galerkin* condition) or to another subspace (*Petrov–Galerkin* condition). The dimension of the subspaces is characteristically much smaller than the dimension N of the original space. This results in a system of much smaller dimension than the original system, which can be solved much more cheaply. Various methods differ by the choice of subspaces. For example, modal condensation corresponds to a subspace spanned by eigenvectors. Padé Via Lanczos (PVL) [1,2] corresponds to Krylov subspaces constructed by the Lanczos process [3]. Forced response condensation [4] corresponds to a subspace spanned by precomputed forced responses. The latter two are particular cases of rational Krylov projection methods [5,6] that correspond to subspaces spanned by several Krylov subspaces and that generate multipoint Padé approximations [7,8]. Guyan reduction [9] and Wilson et al.'s analysis [10] may also be viewed as Krylov projection methods with an interpolation point at zero.

Although the authors know of no other error bounds for these methods in the literature, error estimates do exist. For example, Bai and Ye [11] have proposed two error estimates based on an expression for the error specific to PVL. Their error expression consists of a scalar term that can be easily computed iteratively from the Lanczos process and a term involving an inner product. Their first error estimate is based on a bound of the norm of the operator that is guaranteed to hold only in a small interval around the interpolation point σ. This bound of limited range is used as an estimate in a larger interval of interest. Their second estimate is based on heuristically approximating the operator by the identity.

Starting from the same error expression, Slone [12] notes that even if the norm of the operator were known exactly, the estimate would overestimate the error. He therefore proposes to estimate the norm of the operator by using the norm of the transfer function of the reduced system. Skoogh [13] also proposes an estimate based on expressions from the reduced system. Starting from an actual bound of the error that uses the norm $\|(\mathbf{K} - \lambda\mathbf{M})\mathbf{M}\boldsymbol{v}\|_2$, for a constant vector $\boldsymbol{v}$, Skoogh estimated a bound on this norm by the norm of a vector in the space of the reduced system. All of these error estimates have the benefit of being inexpensive to update at each iteration of the Lanczos process and they are often good indicators of the decrease of the actual error.

In this paper, bounds are derived that offer a *guarantee* that the norm of the error is below a given threshold. The focus is on the harmonic response of the dynamic system and approximations obtained by Rayleigh–Ritz condensation methods. These bounds give upper and lower bounds on the response itself at each point in the frequency band of interest. The presentation begins with a description of the problem, the condensation method, and exact expressions of the error. The error bounds are based on an expansion of the response using interior and exterior eigenpairs. The bounds on the eigenpairs are therefore presented before the bounds on the error and the transfer function of the system. The steps to obtain the bounds are grouped into two algorithms that are presented and discussed. Finally, some examples illustrate applications of the bounds.

II. Problem Description

One is interested in computing the response, $\boldsymbol{x}(\lambda)$, that satisfies

$$(\mathbf{K} - \lambda\mathbf{M})\boldsymbol{x}(\lambda) = \boldsymbol{f} \tag{1}$$

in the frequency band $\lambda \in [\lambda_{\min}, \lambda_{\max}]$. An approximation to $\boldsymbol{x}$,

$$\tilde{\boldsymbol{x}}(\lambda) \equiv \mathbf{T}\mathbf{y}(\lambda) \tag{2}$$

is obtained from a Galerkin Rayleigh–Ritz condensation of the system, which yields the reduced system

$$(\boldsymbol{\kappa} - \lambda\boldsymbol{\mu})\mathbf{y}(\lambda) = \mathbf{T}^T\boldsymbol{f} \tag{3}$$

with $\boldsymbol{\kappa} \equiv \mathbf{T}^T\mathbf{K}\mathbf{T}$ and $\boldsymbol{\mu} \equiv \mathbf{T}^T\mathbf{M}\mathbf{T}$. The stiffness matrix $\mathbf{K}$ is positive semidefinite and the mass matrix $\mathbf{M}$ is positive definite. Both matrices are symmetric and $N \times N$, where N is large. The rectangular matrix $\mathbf{T}$ is full-rank. By construction, the matrices $\boldsymbol{\kappa}$ and $\boldsymbol{\mu}$ are positive semidefinite and positive definite, respectively, and both are symmetric.

The interest here is in bounding the error $e(\lambda)$ on the approximation $\tilde{g}(\lambda) \equiv \boldsymbol{c}^T\tilde{\boldsymbol{x}}(\lambda)$ of the transfer function $g(\lambda) \equiv \boldsymbol{c}^T\boldsymbol{x}(\lambda)$,

$$e(\lambda) \equiv g(\lambda) - \tilde{g}(\lambda) \tag{4}$$

The output vector $\boldsymbol{c}$ may extract any linear combination of the components of the vector $\boldsymbol{x}(\lambda)$. For example, the ith component of the response is obtained by $\boldsymbol{c} = \boldsymbol{e}_i$. The error can be expressed in terms of the residual $\mathbf{r}(\lambda)$

$$e(\lambda) = \boldsymbol{c}^T[\boldsymbol{x}(\lambda) - \tilde{\boldsymbol{x}}(\lambda)] = \boldsymbol{c}^T(\mathbf{K} - \lambda\mathbf{M})^{-1}\mathbf{r}(\lambda) \tag{5}$$

where

$$\mathbf{r}(\lambda) \equiv \boldsymbol{f} - (\mathbf{K} - \lambda\mathbf{M})\tilde{\boldsymbol{x}}(\lambda) \tag{6}$$

The bounds on the error thus give the bounds on the transfer function.

III. Bounds on Eigenpairs

One evaluates the error by using eigenpairs of both the original system and the reduced system. The set of eigenpairs $(\boldsymbol{\phi}_n, \lambda_n)$ of the original system is defined by

$$(\mathbf{K} - \lambda_n\mathbf{M})\boldsymbol{\phi}_n = \mathbf{0} \tag{7}$$

and the set of Ritz pairs or eigenpair estimates $(\tilde{\boldsymbol{\phi}}_m, \tilde{\lambda}_m)$ is defined by

$$(\boldsymbol{\kappa} - \tilde{\lambda}_m\boldsymbol{\mu})\hat{\boldsymbol{\phi}}_m = \mathbf{0} \qquad \tilde{\boldsymbol{\phi}}_m \equiv \mathbf{T}\hat{\boldsymbol{\phi}}_m \tag{8}$$

Because the matrices are symmetric and positive- and semipositive definite, the two systems have full sets of eigenvectors, and the eigenvalues and Ritz values are nonnegative real. The exact and approximate eigenvectors are collected in $\boldsymbol{\Phi}$ and $\tilde{\boldsymbol{\Phi}}$, which are assumed mass-orthonormal $\boldsymbol{\Phi}^T\mathbf{M}\boldsymbol{\Phi} = \mathbf{I}$, and $\tilde{\boldsymbol{\Phi}}^T\mathbf{M}\tilde{\boldsymbol{\Phi}} = \mathbf{I}$.

For any vector $\boldsymbol{\psi}_m$ and eigenvalue estimate $\tilde{\lambda}_m$, there is at least one exact eigenvalue, renumbered λ_m without loss of generality, such that ([14], theorem 15.9.1)

$$\tilde{\lambda}_m - \varepsilon_{\lambda,m} \le \lambda_m \le \tilde{\lambda}_m + \varepsilon_{\lambda,m} \tag{9}$$

where

$$\varepsilon_{\lambda,m} \equiv \|\mathbf{M}^{-1/2}\mathbf{s}_m\| = \sqrt{\mathbf{s}_m^T(\mathbf{M}^{-1}\mathbf{s}_m)} \tag{10}$$

and the residual vector $\mathbf{s}_m$ is

$$\mathbf{s}_m \equiv \mathbf{K}\boldsymbol{\psi}_m - \tilde{\lambda}_m \mathbf{M}\boldsymbol{\psi}_m \tag{11}$$

Here, one typically uses the vector $\boldsymbol{\psi}_m = \tilde{\boldsymbol{\phi}}_m$. The interval $[\tilde{\lambda}_m - \varepsilon_{\lambda,m}, \tilde{\lambda}_m + \varepsilon_{\lambda,m}]$ is called a confidence interval. Note that it is usually possible to improve these eigenvalue bounds. For example, improvements exist if there is a one-to-one matching between all eigenvalues and Ritz values in the interval [4,15]. Notably, if all the eigenvalues are approximated below a given frequency, λ_{band}, because the Ritz values approximate the eigenvalues from above,

$$\tilde{\lambda}_m - \varepsilon_{\lambda,m} \le \lambda_m \le \tilde{\lambda}_m \quad \forall\ \lambda_m \le \lambda_{\text{band}} \tag{12}$$

One can also select the optimum vector $\boldsymbol{\psi}_m$ within the subspace colspan ($\mathbf{T}$) [15].

Henceforth, it is assumed that all the eigenpairs with eigenvalues in the interval of interest are univocally approximated by Ritz pairs. This condition can be checked by using Sylvester's Law of Inertia theorem [16] ([14], theorem 3.3.1) to count the number of eigenvalues in the interval of interest $[\lambda_{\min}, \lambda_{\max}]$ and verify that the interval contains the same number of nonoverlapping confidence intervals as the number of actual eigenvalues. One triangular decomposition is then computed at both ends of the band, $(\mathbf{K} - \lambda_s \mathbf{M}) \equiv \mathbf{L}\mathbf{D}\mathbf{L}^T$, for $\lambda_s = \lambda_{\min}, \lambda_{\max}$. Any other method to count the number of interior eigenvalues could be used in place of using Sylvester's Law of Inertia. One denotes by I the set containing the indices of the Ritz values that match the eigenvalues in the interval $[\lambda_{\min}, \lambda_{\max}]$ and one uses the term interior to refer to the corresponding Ritz pairs or eigenpairs.

With this assumption and using the bound on eigenvectors based on the residual vectors [17], one has that for all interior Ritz pairs $i \in I$ there exists a value

$$\|\mathbf{M}^{1/2}(\tilde{\boldsymbol{\phi}}_i - \alpha_i \boldsymbol{\phi}_i)\| \le \varepsilon_{\phi,i} \tag{13}$$

where $\varepsilon_{\phi,i}$ is defined by

$$\varepsilon_{\phi,i} \equiv \frac{\varepsilon_{\lambda,i}}{\min(\{|\tilde{\lambda}_i - \tilde{\lambda}_k - \varepsilon_{\lambda,k}|\}_{k\in I, k\neq i}, \{|\tilde{\lambda}_i - \tilde{\lambda}_k + \varepsilon_{\lambda,k}|\}_{k\in I, k\neq i}, \tilde{\lambda}_i - \lambda_{\min}, \lambda_{\max} - \tilde{\lambda}_i)} \tag{14}$$

IV. Bounds on the Transfer Function

Upper and lower bounds on the transfer function are now derived. The derivation starts from the exact expression of the error in Eq. (5) and uses bounds for all eigenvalues and eigenvectors in an interval $[\lambda_{\min}, \lambda_{\max}]$.

The approach taken here is to separately consider the part of the residual (and of the vector $\boldsymbol{c}$) corresponding to the interior eigenvectors, and its complementary part. Recall that the set I contains the indices of the eigenpairs for which one has individual bounds on the eigenvalues and the eigenvectors. The complementary set of indices is denoted by E and the label exterior is used to refer to the corresponding eigenpairs and Ritz pairs. Note that it is possible for some Ritz values to lie in the interval of interest, but still not correspond to an element of I. This happens if there are more Ritz values than eigenvalues in the interval, in which case the contribution of the extra Ritz pairs must be removed from the approximate solution $\tilde{\boldsymbol{x}}$. For example, if $(\tilde{\boldsymbol{\phi}}_m, \tilde{\lambda}_m)$ is an extra Ritz pair, one can replace $\tilde{\boldsymbol{x}}$ explicitly by

$$\tilde{\boldsymbol{x}}(\lambda) \leftarrow \tilde{\boldsymbol{x}}(\lambda) - \frac{\tilde{\boldsymbol{\phi}}_m \tilde{\boldsymbol{\phi}}_m^T \boldsymbol{f}}{\tilde{\lambda}_m - \lambda} \tag{15}$$

or implicitly by

$$\mathbf{y}(\lambda) \leftarrow \mathbf{y}(\lambda) - \frac{\hat{\boldsymbol{\phi}}_m \hat{\boldsymbol{\phi}}_m^T \mathbf{T}^T \boldsymbol{f}}{\tilde{\lambda}_m - \lambda} \tag{16}$$

and update the approximate transfer function and the residual of Eq. (6) accordingly.

$$\tilde{g}(\lambda) \leftarrow \tilde{g}(\lambda) - \frac{\boldsymbol{c}^T \mathbf{T} \hat{\boldsymbol{\phi}}_m \hat{\boldsymbol{\phi}}_m^T \mathbf{T}^T \boldsymbol{f}}{\tilde{\lambda}_m - \lambda} \tag{17}$$

$$\mathbf{r}(\lambda) \leftarrow \mathbf{r}(\lambda) + (\mathbf{K}\mathbf{T} - \lambda \mathbf{M}\mathbf{T}) \frac{\hat{\boldsymbol{\phi}}_m \hat{\boldsymbol{\phi}}_m^T \mathbf{T}^T \boldsymbol{f}}{\tilde{\lambda}_m - \lambda} \tag{18}$$

From the orthonormality of the modes, $\boldsymbol{\Phi}^T \mathbf{M} \boldsymbol{\Phi} = \mathbf{I}$, one has $(\mathbf{K} - \lambda \mathbf{M})^{-1} = \boldsymbol{\Phi}(\boldsymbol{\Lambda} - \lambda \mathbf{I})^{-1} \boldsymbol{\Phi}^T$. Using this representation in the error expression of Eq. (5) gives

$$e(\lambda) = e_I(\lambda) + e_E(\lambda) \tag{19}$$

where

$$e_S(\lambda) \equiv \boldsymbol{c}^T \boldsymbol{\Phi}_S (\boldsymbol{\Lambda}_S - \lambda \mathbf{I})^{-1} \boldsymbol{\Phi}_S^T \mathbf{r}(\lambda) \quad \text{for } S = I, E \tag{20}$$

The subscripts I or E denote the submatrices made of interior or exterior eigenpairs, respectively.

A. Bounds on the Interior Error

Considering the two error terms, one expresses the interior error as

$$e_I(\lambda) = \sum_{i\in I} \boldsymbol{\phi}_i^T \boldsymbol{c} \frac{1}{\lambda_i - \lambda} \boldsymbol{\phi}_i^T \mathbf{r}(\lambda) \tag{21}$$

Recall that there is an assumed one-to-one matching between each interior approximation $(\tilde{\boldsymbol{\phi}}_i, \tilde{\lambda}_i)$ and each actual interior eigenpair $(\boldsymbol{\phi}_i, \lambda_i)$, and that the corresponding error bounds are available. One now describes upper and lower bounds individually for the three factors $\boldsymbol{\phi}_i^T \boldsymbol{c}$, $\boldsymbol{\phi}_i^T \mathbf{r}(\lambda)$, and $(\lambda_i - \lambda)^{-1}$. Bounds on the product of the three factors are then directly available. Summing these for all interior eigenpairs gives upper and lower bounds for the interior error. If the assumption of a one-to-one matching is violated, then the error bound is defined to be infinite.

First, from inequality Eq. (9), one has the following bounds on $(\lambda_i - \lambda)^{-1}$ for all $\lambda < \tilde{\lambda}_i - \varepsilon_{\lambda,i}$ and for all $\lambda > \tilde{\lambda}_i + \varepsilon_{\lambda,i}$,

$$\frac{1}{\tilde{\lambda}_i + \varepsilon_{\lambda,i} - \lambda} \le \frac{1}{\lambda_i - \lambda} \le \frac{1}{\tilde{\lambda}_i - \varepsilon_{\lambda,i} - \lambda} \tag{22}$$

From inequality Eq. (12), this inequality simplifies in case of low-frequency band

$$\frac{1}{\tilde{\lambda}_i - \lambda} \le \frac{1}{\lambda_i - \lambda} \le \frac{1}{\tilde{\lambda}_i - \varepsilon_{\lambda,i} - \lambda} \tag{23}$$

Bounds on $\boldsymbol{\phi}_i^T \boldsymbol{c}$ and $\boldsymbol{\phi}_i^T \mathbf{r}(\lambda)$ result from the general inequality ([15], Appendix A.2.1)

$$|\mathbf{v}^T(\boldsymbol{\phi}_i - \tilde{\boldsymbol{\phi}}_i)| \le \sqrt{\mathbf{v}^T \mathbf{M}^{-1} \mathbf{v}} \sqrt{2 - 2\sqrt{1 - \varepsilon_{\phi,i}^2}} \tag{24}$$

if there exist α_i and $\varepsilon_{\phi,i}$ such that $\|\mathbf{M}^{1/2}(\tilde{\boldsymbol{\phi}}_i - \alpha_i \boldsymbol{\phi}_i)\| \le \varepsilon_{\phi,i}$. Therefore, the bounds are

$$\tilde{\boldsymbol{\phi}}_i^T \boldsymbol{c} - \|\mathbf{M}^{-1/2}\boldsymbol{c}\|\delta_{\phi,i} \le \boldsymbol{\phi}_i^T \boldsymbol{c} \le \tilde{\boldsymbol{\phi}}_i^T \boldsymbol{c} + \|\mathbf{M}^{-1/2}\boldsymbol{c}\|\delta_{\phi,i} \tag{25}$$

and

$$-\|\mathbf{M}^{-1/2}\mathbf{r}(\lambda)\|\delta_{\phi,i} \le \boldsymbol{\phi}_i^T \mathbf{r}(\lambda) \le \|\mathbf{M}^{-1/2}\mathbf{r}(\lambda)\|\delta_{\phi,i} \quad \text{for } i \in I \tag{26}$$

where

$$\delta_{\phi,i} \equiv \sqrt{2 - 2\sqrt{1 - \varepsilon_{\phi,i}^2}} \tag{27}$$

The second expression simplified because $\mathbf{r}(\lambda)$ is orthogonal to $\tilde{\boldsymbol{\phi}}_i$ by the Galerkin condition. The upper and lower bounds on the products of the three factors are based on the maximum and minimum of the eight combinations of products of the individual bounds. The upper bounds on e_I are the sum of the upper bounds of the terms for all interior eigenpairs, and likewise for the lower bounds. Because the bounds in inequality Eq. (26) are opposite, one finally has a bound b_I on the magnitude of the interior error,

$$|e_I(\lambda)| \le b_I(\lambda) \tag{28}$$

with

$$b_I(\lambda) = \sum_{i\in I} \frac{1}{|\tilde{\lambda}_i - \lambda| - \varepsilon_{\lambda,i}} \|\mathbf{M}^{-1/2}\mathbf{r}(\lambda)\|\delta_{\phi,i}\left(\left|\tilde{\boldsymbol{\phi}}_i^T \boldsymbol{c}\right| + \|\mathbf{M}^{-1/2}\boldsymbol{c}\|\delta_{\phi,i}\right) \tag{29}$$

everywhere between the confidence intervals.

In case of low-frequency band, a tighter bound is

$$b_I(\lambda) = \sum_{i\in I} \frac{1}{|\tilde{\lambda}_i - \varepsilon_{\lambda,i}/2 - \lambda| - \varepsilon_{\lambda,i}/2} \times \|\mathbf{M}^{-1/2}\mathbf{r}(\lambda)\|\delta_{\phi,i}\left(\left|\tilde{\boldsymbol{\phi}}_i^T \boldsymbol{c}\right| + \|\mathbf{M}^{-1/2}\boldsymbol{c}\|\delta_{\phi,i}\right) \tag{30}$$

B. Bounds on the Exterior Error

The exterior error

$$e_E(\lambda) \equiv \boldsymbol{c}^T \boldsymbol{\Phi}_E (\boldsymbol{\Lambda}_E - \lambda \mathbf{I})^{-1} \boldsymbol{\Phi}_E^T \mathbf{r}(\lambda) \tag{31}$$

is treated differently because approximations to each individual eigenvector are neither available nor required. The cases of low-frequency band and midfrequency band are considered one after the other. Considering the low-frequency band, $\lambda_{\min} = 0$ and $\lambda_{\max} \equiv \lambda_{\text{band}}$, one starts with a bound on the absolute value of the exterior error from the Cauchy–Schwarz inequality

$$\begin{aligned} |e_E(\lambda)| &= \left\| \boldsymbol{c}^T \boldsymbol{\Phi}_E (\boldsymbol{\Lambda}_E - \lambda \mathbf{I})^{-1/2} (\boldsymbol{\Lambda}_E - \lambda \mathbf{I})^{-1/2} \boldsymbol{\Phi}_E^T \mathbf{r}(\lambda) \right\| \\ &\le \left\| (\boldsymbol{\Lambda}_E - \lambda \mathbf{I})^{-1/2} \boldsymbol{\Phi}_E^T \boldsymbol{c} \right\| \left\| (\boldsymbol{\Lambda}_E - \lambda \mathbf{I})^{-1/2} \boldsymbol{\Phi}_E^T \mathbf{r}(\lambda) \right\| \\ &\le \sqrt{\boldsymbol{c}^T \boldsymbol{\Phi}_E (\boldsymbol{\Lambda}_E - \lambda \mathbf{I})^{-1} \boldsymbol{\Phi}_E^T \boldsymbol{c}} \sqrt{\mathbf{r}(\lambda)^T \boldsymbol{\Phi}_E (\boldsymbol{\Lambda}_E - \lambda \mathbf{I})^{-1} \boldsymbol{\Phi}_E^T \mathbf{r}(\lambda)} \end{aligned} \tag{32}$$

By the assumption of a low-frequency band, the coefficients $\lambda_e - \lambda$, $e \in E$ are all positive and the arguments of the two square roots in the last inequality can be expressed as a sum of products of positive terms

$$\boldsymbol{c}^T \boldsymbol{\Phi}_E (\boldsymbol{\Lambda}_E - \lambda \boldsymbol{I})^{-1} \boldsymbol{\Phi}_E^T \boldsymbol{c} = \sum_{e\in E} \left[\boldsymbol{\phi}_e^T \boldsymbol{c}\right]^2 (\lambda_e - \lambda)^{-1} \tag{33}$$

and

$$\mathbf{r}(\lambda)^T \boldsymbol{\Phi}_E (\boldsymbol{\Lambda}_E - \lambda \boldsymbol{I})^{-1} \boldsymbol{\Phi}_E^T \mathbf{r}(\lambda) = \sum_{e\in E} \left[\boldsymbol{\phi}_e^T \mathbf{r}(\lambda)\right]^2 (\lambda_e - \lambda)^{-1} \tag{34}$$

Using the inequalities

$$0 \le \lambda \le \lambda_{\text{band}} \le \lambda_e \quad \forall\ e \in E \tag{35}$$

one can bound $(\lambda_e - \lambda)^{-1}$ in either of the following two ways,

$$\frac{1}{\lambda_e - \lambda} \le \frac{1}{\lambda_{\text{band}} - \lambda} \equiv e_a(\lambda_e, \lambda)^{-1} \quad \forall\ e \in E \tag{36}$$

$$\frac{1}{\lambda_e - \lambda} \le \frac{1}{\lambda_e - \lambda_{\text{band}}} \equiv e_b(\lambda_e, \lambda)^{-1} \quad \forall\ e \in E \tag{37}$$

The arguments of the two square roots of inequality Eq. (32) can therefore be bounded by the following values

$$\mathbf{v}(\lambda)^T \boldsymbol{\Phi}_E (\boldsymbol{\Lambda}_E - \lambda \mathbf{I})^{-1} \boldsymbol{\Phi}_E^T \mathbf{v}(\lambda) \le \mathbf{v}(\lambda)^T \boldsymbol{\Phi}_E \mathbf{E}_t(\boldsymbol{\Lambda}_E, \lambda)^{-1} \boldsymbol{\Phi}_E^T \mathbf{v}(\lambda) \tag{38}$$

for $\mathbf{v} = \boldsymbol{c}$ or $\mathbf{r}(\lambda)$, $\mathbf{E}_t(\boldsymbol{\Lambda}_E, \lambda) = \text{diag}_{e\in E} e_t(\lambda_e, \lambda)$, and $t = a$ or b. If one defines the two following matrices obtained by extending the diagonal matrices $\mathbf{E}_a$ and $\mathbf{E}_b$ to the whole spectrum,

$$\mathbf{B}_a(\lambda) \equiv \mathbf{M}\boldsymbol{\Phi}\mathbf{E}_a(\boldsymbol{\Lambda}, \lambda)\boldsymbol{\Phi}^T\mathbf{M} = \mathbf{M}\boldsymbol{\Phi}(\lambda_{\text{band}}\mathbf{I} - \lambda\mathbf{I})\boldsymbol{\Phi}^T\mathbf{M} \tag{39}$$

$$= (\lambda_{\text{band}} - \lambda)\mathbf{M} \tag{40}$$

$$\mathbf{B}_b(\lambda) \equiv \mathbf{M}\boldsymbol{\Phi}\mathbf{E}_b(\boldsymbol{\Lambda}, \lambda)\boldsymbol{\Phi}^T\mathbf{M} = \mathbf{M}\boldsymbol{\Phi}(\boldsymbol{\Lambda} - \lambda_{\text{band}}\mathbf{I})\boldsymbol{\Phi}^T\mathbf{M} \tag{41}$$

$$= (\mathbf{K} - \lambda_{\text{band}}\mathbf{M}) \tag{42}$$

then the bounds of inequality Eq. (38) can be expressed as

$$\begin{aligned} \mathbf{v}(\lambda)^T \boldsymbol{\Phi}_E \mathbf{E}_t(\boldsymbol{\Lambda}_E, \lambda)^{-1} \boldsymbol{\Phi}_E^T \mathbf{v}(\lambda) &= \mathbf{v}(\lambda)^T \mathbf{B}_t(\lambda)^{-1} \mathbf{v}(\lambda) \\ &\quad - \mathbf{v}(\lambda)^T \boldsymbol{\Phi}_I \mathbf{E}_t(\boldsymbol{\Lambda}_I, \lambda)^{-1} \boldsymbol{\Phi}_I^T \mathbf{v}(\lambda) \end{aligned} \tag{43}$$

for $\mathbf{v} = \boldsymbol{c}$ or $\mathbf{r}(\lambda)$ and $t = a$ or b. These bounds can themselves be bounded relatively cheaply by

$$\mathbf{v}(\lambda)^T \boldsymbol{\Phi}_E \mathbf{E}_t(\boldsymbol{\Lambda}_E, \lambda)^{-1} \boldsymbol{\Phi}_E^T \mathbf{v}(\lambda) \le \mathbf{v}(\lambda)^T \mathbf{B}_t(\lambda)^{-1} \mathbf{v}(\lambda) - S[\mathbf{E}_t, \mathbf{v}(\lambda)] \tag{44}$$

Here, $S[\mathbf{E}_t, \mathbf{v}(\lambda)]$ denotes a lower bound on the scalar

$$\sum_{i\in I} \mathbf{E}_t(\lambda_i, \lambda)^{-1} \left[\boldsymbol{\phi}_i^T \mathbf{v}(\lambda)\right]^2$$

$$S[\mathbf{E}_t, \mathbf{v}(\lambda)] \le \sum_{i\in I} \mathbf{E}_t(\lambda_i, \lambda)^{-1} \left[\boldsymbol{\phi}_i^T \mathbf{v}(\lambda)\right]^2 \tag{45}$$

Again, $\mathbf{v}(\lambda) = \boldsymbol{c}$ or $\mathbf{r}(\lambda)$ and $t = a$ or b.

Inequalities Eqs. (22), (25), and (26) can be used to compute S for each of the four cases considered:

$$S(\mathbf{E}_a, \boldsymbol{c}) = \frac{1}{4(\lambda_{\text{band}} - \lambda)} \sum_{i\in I} \left[\left| \left(\left| \tilde{\boldsymbol{\phi}}_i^T \boldsymbol{c} \right| - \|\mathbf{M}^{-1/2}\boldsymbol{c}\|\delta_{\phi,i} \right) \right| + \left| \tilde{\boldsymbol{\phi}}_i^T \boldsymbol{c} \right| - \|\mathbf{M}^{-1/2}\boldsymbol{c}\|\delta_{\phi,i} \right]^2 \tag{46}$$

$$S[\mathbf{E}_a, \mathbf{r}(\lambda)] = 0 \tag{47}$$

$$S(\mathbf{E}_b, \boldsymbol{c}) = -\sum_{i\in I} \frac{1}{\lambda_{\text{band}} - \tilde{\lambda}_i} \left(\left| \tilde{\boldsymbol{\phi}}_i^T \boldsymbol{c} \right| + \|\mathbf{M}^{-1/2}\boldsymbol{c}\|\delta_{\phi,i} \right)^2 \tag{48}$$

$$S[\mathbf{E}_b, \mathbf{r}(\lambda)] = -\sum_{i\in I} \frac{1}{\lambda_{\text{band}} - \tilde{\lambda}_i} \mathbf{r}(\lambda)^T \mathbf{M}^{-1} \mathbf{r}(\lambda) \delta_{\phi,i}^2 \tag{49}$$

Putting together the bounds just discussed gives

$$|e_E(\lambda)| \le b_E(\lambda) = \sqrt{\mathbf{r}(\lambda)^T \mathbf{B}_t^{-1} \mathbf{r}(\lambda) - S[\mathbf{E}_t, \mathbf{r}(\lambda)]} \cdot \sqrt{\boldsymbol{c}^T \mathbf{B}_t^{-1} \boldsymbol{c} - S(\mathbf{E}_t, \boldsymbol{c})} \tag{50}$$

for $t = a$ or b.

In the general case of a frequency band in the midfrequency range, $\lambda_e - \lambda$ is either positive or negative. One can consider

$$\begin{aligned} |e_E(\lambda)| &= \left\| \boldsymbol{c}^T (\boldsymbol{\Lambda}_E - \lambda \mathbf{I})^{-1} \boldsymbol{\Phi}_E^T \mathbf{r}(\lambda) \right\| \\ &\le \left\| \boldsymbol{\Phi}_E^T \boldsymbol{c} \right\| \left\| (\boldsymbol{\Lambda}_E - \lambda \mathbf{I})^{-1} \boldsymbol{\Phi}_E^T \mathbf{r}(\lambda) \right\| \\ &\le \sqrt{\boldsymbol{c}^T \boldsymbol{\Phi}_E \boldsymbol{\Phi}_E^T \boldsymbol{c}} \sqrt{\mathbf{r}(\lambda)^T \boldsymbol{\Phi}_E (\boldsymbol{\Lambda}_E - \lambda \mathbf{I})^{-2} \boldsymbol{\Phi}_E^T \mathbf{r}(\lambda)} \end{aligned} \tag{51}$$

One notes

$$[\min(\lambda - \lambda_{\min}, \lambda_{\max} - \lambda)]^2 \le (\lambda_e - \lambda)^2 \quad \forall\ e \in E \tag{52}$$

Proceeding in a manner analogous to that of the preceding case a gives

$$|e_E(\lambda)| \le b_E(\lambda) \tag{53}$$

with

$$b_E(\lambda) = \frac{\sqrt{\mathbf{r}(\lambda)^T \mathbf{M}^{-1} \mathbf{r}(\lambda)}}{\min(\lambda - \lambda_{\min}, \lambda_{\max} - \lambda)} \cdot \sqrt{\boldsymbol{c}^T \mathbf{M}^{-1} \boldsymbol{c} - S(\mathbf{I}, \boldsymbol{c})} \tag{54}$$

$S(\mathbf{I}, \boldsymbol{c})$ denotes a lower bound on the scalar $\sum_{i\in I} [\boldsymbol{\phi}_i^T \boldsymbol{c}]^2$. Specifically,

$$S(\mathbf{I}, \boldsymbol{c}) = \frac{1}{4} \sum_{i\in I} \left[\left| \left(\left| \tilde{\boldsymbol{\phi}}_i^T \boldsymbol{c} \right| - \|\mathbf{M}^{-1/2} \boldsymbol{c}\| \delta_{\phi,i} \right) \right| + \left| \tilde{\boldsymbol{\phi}}_i^T \boldsymbol{c} \right| - \|\mathbf{M}^{-1/2} \boldsymbol{c}\| \delta_{\phi,i} \right]^2 \tag{55}$$

The matrix corresponding to the previous matrices $\mathbf{B}_a$ and $\mathbf{B}_b$ is

$$\mathbf{B}_m(\lambda) \equiv \min(\lambda - \lambda_{\min}, \lambda_{\max} - \lambda) \mathbf{M} \tag{56}$$

C. Bounds on the Total Error and the Transfer Function

Combining the upper bounds on the magnitude of the interior error, inequality Eq. (28), and of the exterior error, inequalities Eq. (50) or Eq. (53), one has bounds on the total error and on the transfer function everywhere between the confidence intervals

$$|e(\lambda)| \le b_I(\lambda) + b_E(\lambda) \tag{57}$$

and

$$\tilde{g}(\lambda) - b_I(\lambda) - b_E(\lambda) \le g(\lambda) \le \tilde{g}(\lambda) + b_I(\lambda) + b_E(\lambda) \tag{58}$$

The reader can easily verify that the error bound is zero if the error is zero. Indeed, the residual in the various bounds is zero in this case.

V. Algorithmic Considerations

The preceding presentation results in a number of steps to generate the bounds on the transfer function. These steps are structured into two algorithms. Algorithm 1 accomplishes three things. It defines a

Algorithm 1 Bounds on eigenpairs

INPUT:	The original matrices $\mathbf{K}$ and $\mathbf{M}$; The transformation matrix $\mathbf{T}$ and the reduced matrices $\boldsymbol{\kappa}$ and $\boldsymbol{\mu}$; The interval of interest $[\lambda_{\min}, \lambda_{\max}]$.
OUTPUT	The set I of interior eigenpairs; The bounds on the interior eigenpairs, $\varepsilon_{\lambda,i}$ and $\varepsilon_{\phi,i}$ for all $i \in I$; The updated approximate transfer function $\tilde{g}(\lambda)$.
1.	Compute the approximations $\tilde{\boldsymbol{\phi}}_n, \tilde{\lambda}_n$ from the reduced system as defined in Eq. (8).
2.	Compute the bounds $\varepsilon_{\lambda,n}$ for all eigenvalue estimates in the band from Eq. (10).
3.	Evaluate the number of eigenvalues in the band by using Sylvester's inertia theorem.
4.	Verify that the number of eigenvalues in the band equals the number of nonoverlapped confidence intervals contained entirely in the band. Create a set I containing the indices of these confidence intervals. If some Ritz values are in the band but are not part of the interior set, subtract the contribution of their eigenpairs from the approximate transfer function as shown in Eq. (17). Create a set E complementary to the set I.
5.	Optionally, improve the eigenvalue bounds $\varepsilon_{\lambda,i}$ by using the approximation of the distance to the closest eigenvalues [4].
6.	Compute the bounds $\varepsilon_{\phi,i}$ for all interior eigenvector estimates from Eq. (14).

Algorithm 2 Bounds on transfer function

INPUT:	The approximate interior eigenpairs $(\tilde{\lambda}_i, \tilde{\boldsymbol{\phi}}_i)$ and their bounds $\varepsilon_{\lambda,i}$ and $\varepsilon_{\phi,i}$, $i \in I$; The interval of interest $[\lambda_{\min}, \lambda_{\max}]$; The original matrices $\mathbf{K}, \mathbf{M}$; The output and residual vectors $\boldsymbol{c}$ and $\mathbf{r}(\lambda)$; The updated approximate transfer function $\tilde{g}(\lambda)$.
OUTPUT:	The bound on the magnitude of the interior error $b_I(\lambda)$; The bound on the magnitude of the exterior error $b_E(\lambda)$; The upper and lower bounds on the total error and on the transfer function.
1.	Compute the bound on the magnitude of the interior error: a) compute the bounds on the three factors for all $i \in I$ from inequality Eq. (22), and inequality Eqs. (25) and (26), b) get upper bounds on the product of these three factors for all $i \in I$ by taking the maximum among the eight possible products of individual bounds, c) sum the upper bounds for all $i \in I$ to get the bound on the magnitude of the interior error.
2.	Compute the bound on the magnitude of the exterior error: a) compute the bounds $S(\mathbf{E}_a, \boldsymbol{c})$, $S(\mathbf{E}_b, \boldsymbol{c})$, $S[\mathbf{E}_b, \mathbf{r}(\lambda)]$, or $S(\mathbf{I}, \boldsymbol{c})$ from Eq. (46), Eqs. (48) and (49), and Eq. (55), b) compute the bounds on the magnitude of the exterior error from inequality Eq. (50) or inequality Eq. (53).
3.	Compute the bounds on the magnitude of the whole error and on the transfer function from inequality Eqs. (57) and (58).

Algorithm 3 Preprocessing to compute the norms of the output and residual vectors

Preprocessing

1. Compute and store the matrix products:
   a) $\mathbf{T_K} \equiv \mathbf{KT}$,
   b) $\mathbf{T_M} \equiv \mathbf{MT}$.
2. Compute and store the solutions:
   a) $\mathbf{z}_f \equiv \mathbf{M^{-1}}\boldsymbol{f}$,
   b) $\mathbf{z}_c \equiv \mathbf{M}^{-1}\boldsymbol{c}$,
   c) $\mathbf{z}_{\mathbf{T_K}} \equiv \mathbf{M}^{-1}\mathbf{T_K}$.

Use of preprocessing results

1. Compute the vectors:
   a) $\mathbf{r}(\lambda) = \boldsymbol{f} - \mathbf{T_K}\mathbf{y}(\lambda) + \lambda\mathbf{T_M}\mathbf{y}(\lambda)$,
   b) $\mathbf{M}^{-1}\mathbf{r}(\lambda) = \mathbf{z}_f - \mathbf{z}_{\mathbf{T_K}}\mathbf{y}(\lambda) + \lambda\mathbf{T}\mathbf{y}(\lambda)$.
2. Compute the inner product of these to get
   $\|\mathbf{M}^{-1/2}\mathbf{r}(\lambda)\|^2 = \mathbf{r}(\lambda)^T\mathbf{M}^{-1}\mathbf{r}(\lambda)$.

set I if all interior eigenvalues are well approximated, updates the approximation if necessary, and returns bounds on the interior eigenpairs. Algorithm 2 returns the upper and lower bounds on the transfer function for any value of $\lambda \in [\lambda_{\min}, \lambda_{\max}]$. The bounds in the interior confidence intervals $\tilde{\lambda}_i - \varepsilon_{\lambda,i} \le \lambda \le \tilde{\lambda}_i + \varepsilon_{\lambda,i}$ for all $i \in I$ are infinite because the eigenvalues can be anywhere there.

Two general remarks can be made regarding the efficient implementation of the algorithms. First, some expressions appear several places in the computation of the bounds; these need to be evaluated only once. For example, $\|\mathbf{M}^{-1/2}\mathbf{c}\|$ appears both in inequality Eq. (25) and in Eq. (54). Second, the λ dependence of terms including $\mathbf{r}(\lambda)$ can be greatly simplified. For example, instead of computing $\mathbf{M}^{-1}\mathbf{r}(\lambda)$ directly for each value of λ, it is possible to apply $\mathbf{M}^{-1}$ to a subspace of small dimension that is independent of λ. This last fact is because $\mathbf{r}(\lambda)$ is in a subspace of relatively small dimension. Some potential large economy can be seen by the expansion of $\|\mathbf{M}^{-1/2}\mathbf{r}(\lambda)\|^2 = \mathbf{r}^T(\lambda)\mathbf{M}^{-1}\mathbf{r}(\lambda)$ into

$$\begin{aligned}\mathbf{r}(\lambda)^T\mathbf{M}^{-1}\mathbf{r}(\lambda) &= \boldsymbol{f}^T\mathbf{M}^{-1}\boldsymbol{f} - 2\boldsymbol{f}^T\mathbf{M}^{-1}\mathbf{KT}\mathbf{y}(\lambda)\\ &+ \mathbf{y}(\lambda)^T\mathbf{T}^T\mathbf{K}\mathbf{M}^{-1}\mathbf{KT}\mathbf{y}(\lambda) + 2\lambda\mathbf{T}^T\boldsymbol{f}^T\mathbf{y}(\lambda)\\ &- 2\lambda\mathbf{y}(\lambda)^T\boldsymbol{\kappa}\mathbf{y}(\lambda) + \lambda^2\mathbf{y}(\lambda)^T\boldsymbol{\mu}\mathbf{y}(\lambda)\end{aligned} \tag{59}$$

The scalar $\boldsymbol{f}^T\mathbf{M}^{-1}\boldsymbol{f}$, the vector $\boldsymbol{f}^T\mathbf{M}^{-1}\mathbf{KT}$, and the matrix $\mathbf{T}^T\mathbf{K}\mathbf{M}^{-1}\mathbf{KT}$ are independent of λ and have small dimension. Further economy could be achieved by using the modal expansion of $\mathbf{y}(\lambda)$ in these expressions

$$\mathbf{y}(\lambda) = \sum_m \frac{\hat{\boldsymbol{\phi}}_m\hat{\boldsymbol{\phi}}_m^T\mathbf{T}^T\boldsymbol{f}}{\tilde{\lambda}_m - \lambda} \tag{60}$$

which highlights the minimal λ dependence, $(\tilde{\lambda}_m - \lambda)^{-1}$.

The value of the expressions independent of λ could be computed once before running the algorithms or, like the repeated terms, they could be stored when they first appear. An efficient implementation of the algorithms might therefore include a preprocessing phase, whose results are stored and used later. For example, Algorithm 3 shows one particular choice of preprocessing phase used to compute the norms of the output and the residual vectors. Note that all the solutions involving $\mathbf{M}$ are gathered in step 2 of the preprocessing phase, which might allow the storage and reuse of a factorization of $\mathbf{M}$ or an iterative solve with all the right-hand side vectors handled together in a block matrix.

Optimal implementation of the error bound algorithms depends intimately on the condensation method and on the context in which it is used. For example, if the method is a Krylov projection method [5], most of the expressions can be iteratively updated when the dimension of the subspace is increased. The generation and propagation of precision loss due to finite precision calculations should also be considered for a particular condensation method.

VI. Numerical Examples

In this section, the authors present and comment on the application of the bounds to three different reduction methods applied to three different problems with two different force vectors. Both low-frequency and midfrequency bands are considered, and the error bounds are compared with the exactly computed error in each case. Two bounds are available at low frequency, generated from either $\mathbf{B}_a$ or $\mathbf{B}_b$; the bound from $\mathbf{B}_m$ is used in midfrequency. The intent is to give a picture from a broad range of situations of how the bounds typically perform.

A. Description of the Problems

The problems are from the dynamic analysis sets of the public Harwell–Boeing collection of matrices [18]. Three pairs of stiffness and mass matrices of varying sizes have been chosen. They are described in Table 1, in which the model name BCSSTn refers to the stiffness and lumped mass matrices BCSSTKn and BCSSTMn, respectively. The matrices can be found in *The Matrix Market* [19], a service of the National Institute of Standards and Technology.

The output of interest is the first unit vector, $\boldsymbol{c} = \boldsymbol{e}_1 = [1, 0, \ldots, 0]^T$, whereas the force vector is either the first unit vector $\boldsymbol{f} = \boldsymbol{c} = \boldsymbol{e}_1$, or the vector whose coefficients are all one $\boldsymbol{f} = \mathbf{a} = [1, 1, \ldots, 1]^T$.

Considered are both low-frequency or midfrequency bands whose edges, as well as the number of interior eigenvalues N_i, are described in Table 2 for the three problems.

B. Description of the Reduction Methods

Three reduction methods have been chosen on which to test the error bounds presented earlier. The range of methods was chosen to test the performance of the error bounds in a broad spectrum of possible applications.

1. Modal Condensation

This is probably the most common condensation method used in structural dynamics. It proceeds in two steps. First, several of the lowest frequency eigenpairs are computed. Second, these eigenvectors are used in a modal condensation approximation of the transfer function. Although it seems obvious that all eigenpairs with eigenvalues in the band should be computed and used in the approximation, the selection of eigenpairs with eigenvalues outside the band that are used in the approximation is effectively done on an arbitrary basis and heuristics are used. For example, a common heuristic consists in computing and using all the eigenpairs with eigenvalues below a multiple (e.g., three times) of the low-band frequency. Another commonly used heuristic is based on a computation of the modal mass. A third heuristic is based on measuring the change in the approximation with increasing model

Table 1 Description of the problems

Model name	Description	Size	Number of nonzero coefficients
BCSST11	ore car	1473	34,241
BCSST24	Calgary Olympic Saddledome Arena	3562	159,912
BCSST25	Columbia Center 76-story skyscraper	15,439	252,241

Table 2 Description of the bands of interest

Problem	λ_{band}	N_i	$\lambda_{\min}$	$\lambda_{\max}$	N_i
BCSST11	2000	26	4000	6000	9
BCSST24	250	76	4000	6000	15
BCSST25	——	——	950	1050	79

size. For example, if the predicted response with 30 vectors remains unchanged when computed with 40 vectors, the approximation is thought to be accurate. When using such heuristics, however, it is difficult to be sure that an adequate number of eigenpairs has been included to obtain an accurate approximation of the transfer function. The error bounds presented in this paper can give a quantitative assessment of the quality of the approximation as a function of M, the number of retained eigenvectors. Furthermore, not only do the error bounds allow one to check whether a particular approximation is accurate enough, they also allow one to identify when one can stop increasing the dimension of the reduced model in an iterative process.

Regarding the application of the bounds to this case, in which all the smallest eigenvalues are computed, there is no need to count the number of interior eigenvalues. Furthermore, one can obtain a tighter bound if one uses the largest known eigenvalue instead of λ_{band} in the expression of $\mathbf{B}_a$ in Eq. (39). This substitution is made in the examples.

2. *Ritz Vector Condensation*

Instead of computing the eigenpairs very precisely, one could compute the interior Ritz pairs only accurately enough such that the confidence intervals are within a radius $\epsilon \equiv \delta\lambda_{\text{band}}/N_I$ from their Ritz values. Here, δ is a small tolerance, which is chosen to be $\delta = 0.01$ in the following examples. In practice, it makes sense to choose δ in accordance with the accuracy of the spatial discretization used in the original finite element method (FEM) model. (That is, for a given mesh, the discrete eigenvalues will be within a predictable tolerance of the eigenvalues in the exact continuous problem. It would be a waste of computational resources to make δ significantly smaller than this tolerance.) The accuracy of the approximation can be improved by adding Ritz pairs with Ritz values lying outside the interval, independent of whether they accurately approximate eigenpairs.

This procedure is followed in the examples given next. Thus, the second method consists of an approximate modal condensation at low frequency using the Ritz pairs with smallest Ritz values. The Ritz pairs are extracted from a single Krylov subspace at $\sigma = 0$. The chosen dimension of the Krylov subspace is the smallest value such that all the interior eigenvalues are approximated, their confidence intervals do not overlap, and they are within the radius ϵ from the Ritz values. The size of the reduced model is equal to the number of Ritz pairs used in the approximation.

3. *Krylov Projection Method*

The third method is a Krylov projection method. The system is projected onto a single Krylov subspace $\mathcal{K}_M[(\mathbf{K} - \sigma\mathbf{M})^{-1}\mathbf{M}, (\mathbf{K} - \sigma\mathbf{M})^{-1}\boldsymbol{f}]$ of increasing dimension M. The frequency parameter σ is chosen to be the center of the band, i.e., $\sigma = \lambda_{\text{band}}/2$ or $\sigma = (\lambda_{\min} + \lambda_{\max})/2$ for the low-frequency or the midfrequency bands, respectively. The size of the reduced model is equal to the dimension of the Krylov subspace. A Lanczos method is used to generate a basis of the Krylov subspaces.

C. Description of the Results

All the calculations have been done using Matlab.[§] The first example corresponds to bounds on a modal condensation approximation at low frequency. The other examples explore the effect of changes with the method of approximation, the frequency band and the problem. The response in frequency is presented for the first example. In other examples, one finds it useful to use an integral norm of the error and the bound.

It is clear that almost any reasonable measure of the error over the selected frequency band will be infinite if even just one of the eigenvalues is inaccurately approximated. Consequently, the error bounds are infinite unless each eigenvalue in the frequency band of interest is sufficiently well approximated. Beyond that point, adding additional vectors to the condensation subspace may substantially improve the accuracy of the approximation overall in the frequency band. To define an overall integrated measure of the error, one chooses an L_2 measure over the frequency band, excluding regions in which the error and/or the bound is pointwise infinite. That is, small regions around the computed Ritz values and at the band edges are excluded. Thus, one measures the magnitude of the function f ($f = e, b$; f is either the exact error or an error bound) as a function of M, the size of the reduced model, as

$$I_{2,\text{rel}}(f) \equiv \frac{I_2(f)}{I_2(\tilde{g})} \tag{61}$$

$$I_2(f) \equiv \int_{B_{\text{finite}}} f(\lambda)^2 \, \mathrm{d}\lambda \tag{62}$$

Here, B_{finite} represents the whole frequency band except for the intervals of radius $\epsilon \equiv \delta(\lambda_{\max} - \lambda_{\min})/N_I$ around each interior Ritz value, the interval above the largest interior eigenvalue or Ritz value, whichever is the largest, and, for the midfrequency range only, the interval below the smallest interior eigenvalue or Ritz value, whichever is the smallest. The values of the integrals are either infinite, in which case an arbitrary high value 10^{10} is shown in the plots, or finite, in which case the value is evaluated numerically by a trapezoidal integration schema. The functional $I_{2,\text{rel}}(\cdot)$ is labeled "relative L2-norm" in the figures to follow.

D. Baseline Example at Low Frequency

The approximation by modal condensation using the 26 interior eigenpairs is shown in Fig. 1 for the problem BCSST11 at low frequency with $\boldsymbol{f} = \boldsymbol{e}_1$. The error magnitude is about one order of magnitude larger than the approximation itself in most of the band. This approximation is clearly inadequate and needs to be refined. This fact is indicated by both of the error bounds shown in Fig. 1. Furthermore, the more accurate bound (b) provides both a bound *and* an accurate estimate of the exact error. Also, because the bounds are bounds, it is easy to select the more accurate of the two by simply taking the smaller value.

The sharpness of bound b is essentially due to two factors. First, the angle between the vectors $(\boldsymbol{\Lambda}_E - \lambda\mathbf{I})^{-1/2}\boldsymbol{\Phi}_E^T\boldsymbol{c}$ and $(\boldsymbol{\Lambda}_E - \lambda\mathbf{I})^{-1/2}\boldsymbol{\Phi}_E^T\mathbf{r}(\lambda)$ is very small for $\boldsymbol{c} = \boldsymbol{f}$. This is generally true for any condensation method. It should even be analytically zero for a modal condensation method. Because the angle is small, the bound introduced in inequality Eq. (32) is tight. Second, the further the exterior eigenvalues λ_e are from the band, the tighter the bounds in inequality Eq. (37) are. The exterior eigenvalues are relatively far

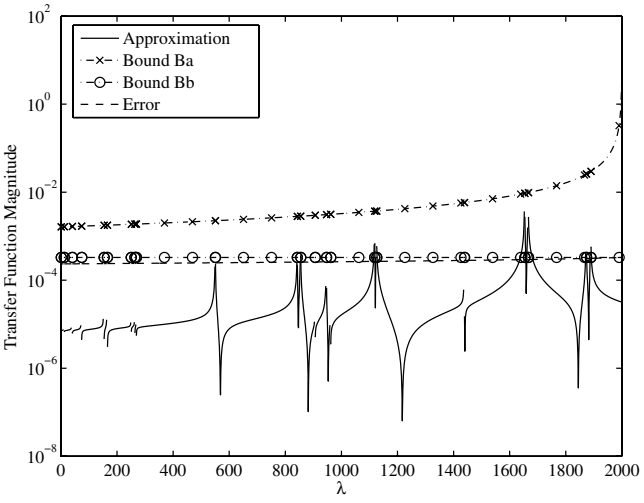

Fig. 1 Low-frequency band example BCSST11 with $\boldsymbol{f} = \boldsymbol{e}_1$ using the 26 interior eigenpairs only.

[§]MathWorks, Inc., Matlab 7.0.1.24704 Release 14.

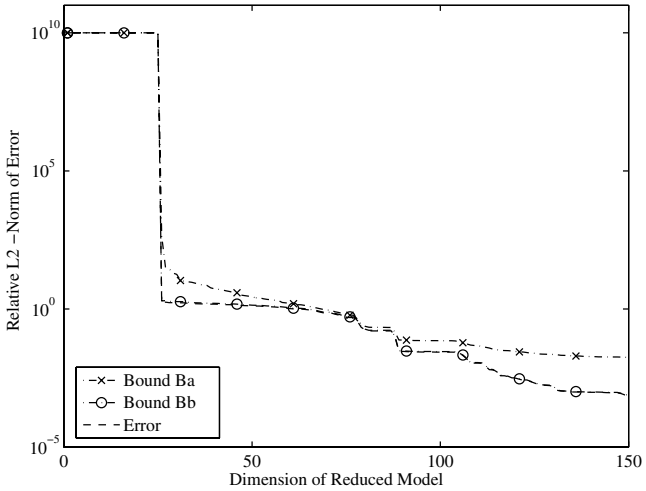

Fig. 2 Integrated error bound $I_{2,\mathrm{rel}}$ vs model size for modal condensation. Low-frequency band example BCSST11. The force vector is $f = e_1$.

from the band for this problem. For problems with exterior eigenvalues relatively close to the band, it would be the bound a which would give very tight bounds.

Figure 2 shows the integrated error as a function of the size of the reduced model. The behavior of the two bounds clearly mimics the behavior of the exact error magnitude when the size of the reduced model is increased. The same is true for other condensation methods and other force vectors. This is shown in the next section.

Incidental to illustrating one application of the bounds, this example stresses also the fact that the bounds on the transfer function need to consider both the interior and exterior errors. Indeed, even if the interior eigenpairs are known, the magnitude of the error in most of the band is still one order larger than the magnitude of the transfer function itself. Without the complete bounds, it would be difficult to know if the approximation is accurate or not.

E. Variations on the Baseline Example

If the force vector differs from the output vector, the angle between the two vectors of inequality Eq. (32) is larger and the bound is therefore less sharp. Even though the force vector $\boldsymbol{f} = [1, \ldots, 1]^T$ makes a large angle, $\arccos(\sqrt{1/1473}) = 88.5\,\mathrm{deg}$, with the output vector $\boldsymbol{c} = [1, 0, \ldots, 0]$, the behavior of the bounds follows the behavior of the error as can be seen in Fig. 3. One can see, for example, that the overall error decreases agonizingly slowly with

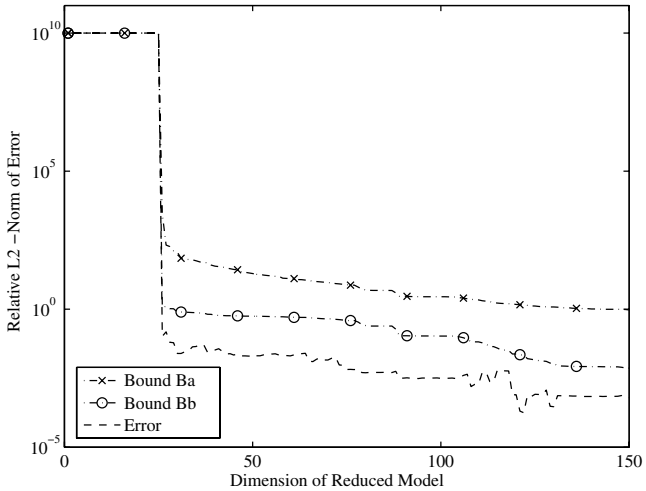

Fig. 3 Integrated error bound $I_{2,\mathrm{rel}}$ vs model size for modal condensation and different force vector. Low-frequency band example BCSST11. The force vector is $f = \mathrm{a}$.

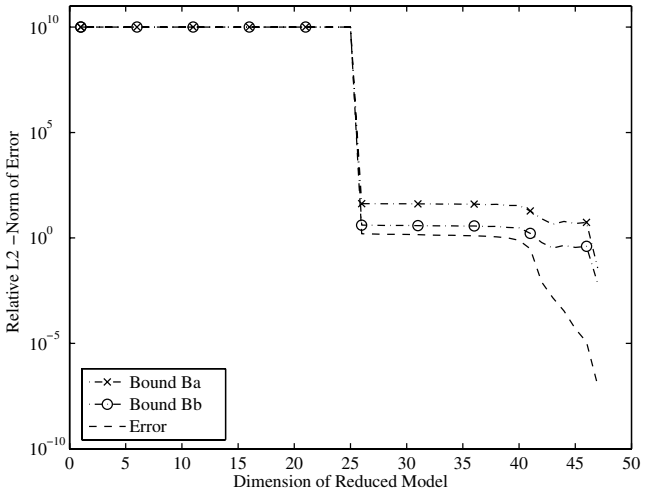

Fig. 4 Integrated error bound $I_{2,\mathrm{rel}}$ vs model size for Ritz vector condensation. Low-frequency band example BCSST11. The force vector is $f = e_1$.

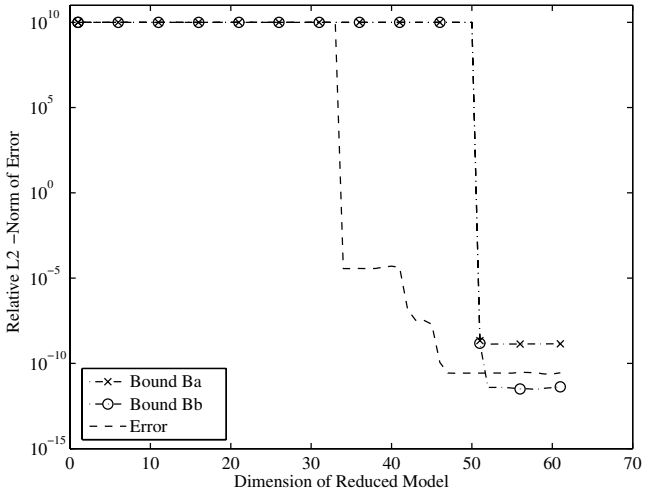

Fig. 5 Integrated error bound $I_{2,\mathrm{rel}}$ vs model size for Krylov projection method. Low-frequency band example BCSST11. The force vector is $f = e_1$.

model size. The rate of decrease with model size is accurately reflected in both bounds.

Although bounds, by their nature, overestimate the error, they are still useful in practical application. In this problem, for example, bound b predicts for a model size of 26 the relative error to be below $\mathcal{O}(10)$, i.e., it predicts that the approximation is useless. The actual relative error there is $\mathcal{O}(1)$, which shows that indeed, the approximation is useless. For a model size of 140 modes, bound b guarantees a relative error below about 5×10^{-2}, whereas the exact error there is about 5×10^{-3}; certainly below, but tolerably close to the lower bound.

Finally, one notes that both the exact error and bound b are characterized by several plateaus, within which the response remains

Table 3 Low-frequency band example BCSST11; case $f = [1, 0, \ldots, 0]$; history of iterations when using a single Krylov subspace at $\sigma = \lambda_{\mathrm{band}}/2$

Dimension of approximation	N_{miss}	N_{prec}
26	7	10
30	5	12
35	4	14
40	2	17
45	0	20
50	0	26

substantially unchanged. If one were using a heuristic based on computed change in the response with M, without error bounds, one might be deceived into thinking a reduced model is accurate as soon as the first plateau is reached, regardless of the level of that plateau.

The bounds also perform well when the approximation is obtained by other reduction methods, as is illustrated for the Ritz vector condensation and the Krylov projection method in Figs. 4 and 5, respectively. The history of the iterations for the projection methods is presented in Table 3. The error in the Ritz reduction method displays two distinct trends. Initially (for about $26 < M < 40$), the Ritz vectors provide accurate approximations of the matrix eigenvectors and both the exact error and the bounds drop slowly as in the modal condensation. Above $M \approx 40$, both the exact error and the error bounds begin falling off more quickly. Finally, at $M = 47$, the error drops precipitously to numerical precision, as indicated by all three curves. As in the previous example, the behavior of the bounds accurately mimics the behavior of the error.

The Krylov space reduction method provides yet another type of behavior of the error with model size. Figure 5 shows the error is practically infinite until a model size of about 30, and then drops suddenly to a relatively low value. At this point, however, clusters of unresolved interior eigenvalues are masked by a single Ritz value in the approximation. The missing Ritz values in these clusters are resolved at around 42 and 46, with concomitant drops in the error. The error drops to numerical precision at a model size of about 47. The bounds, on the other hand, drop to numerical precision at a model size of about 51. And so, if one were relying on the bounds in this case to determine when to truncate the model, one would have taken only four more Krylov vectors than absolutely necessary.

The fact that the "integrated error" is not infinite between $M = 30$ and $M = 46$ has more to do with the pathologies of the definition of integrated error and the size of the eigenvalue clusters, than it has to do with the error itself. The fact is that until $M = 47$, the eigenvalues are not univocally approximated and, therefore, some peaks in the response are missed. Those peaks are missed from the "integrated error" measure because they happen to fall into a gap masked by a neighboring Ritz value. And so, it might be argued that in this pathological case, the error bound curve more accurately reflects the behavior of the true error than does the curve of the integrated error.

F. Variation of Model

The behavior of the bounds and the reduction methods presented in the preceding sections are similar for other models. This is illustrated in this section for model BCSST24. The norm of the error as a function of the size of the reduced model is presented in Fig. 6 for modal condensation with the force vector $\boldsymbol{f} = \boldsymbol{e}_1$. Again, the bound b is very tight and both bounds follow the trend of the error. Because of

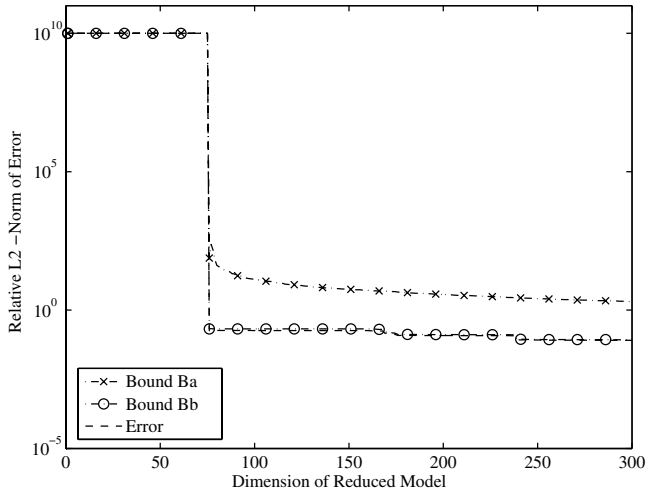

Fig. 6 Integrated error bound $I_{2,\mathrm{rel}}$ vs model size for modal condensation. Low-frequency band example BCSST24. The force vector is $\boldsymbol{f} = \boldsymbol{e}_1$.

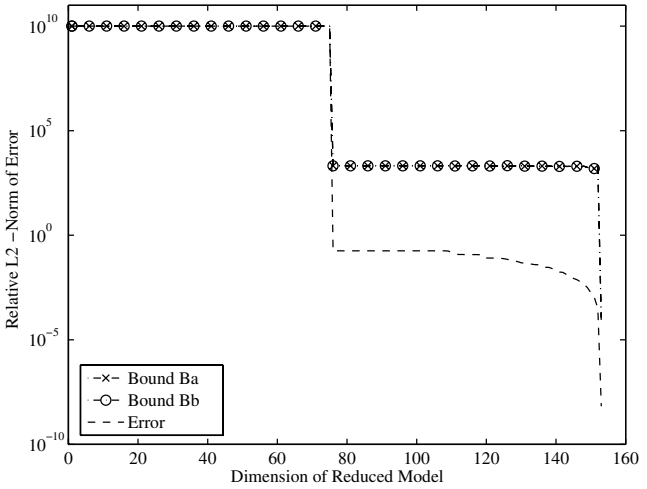

Fig. 7 Integrated error bound $I_{2,\mathrm{rel}}$ vs model size for Ritz vector condensation. Low-frequency band example BCSST24. The force vector is $\boldsymbol{f} = \boldsymbol{e}_1$.

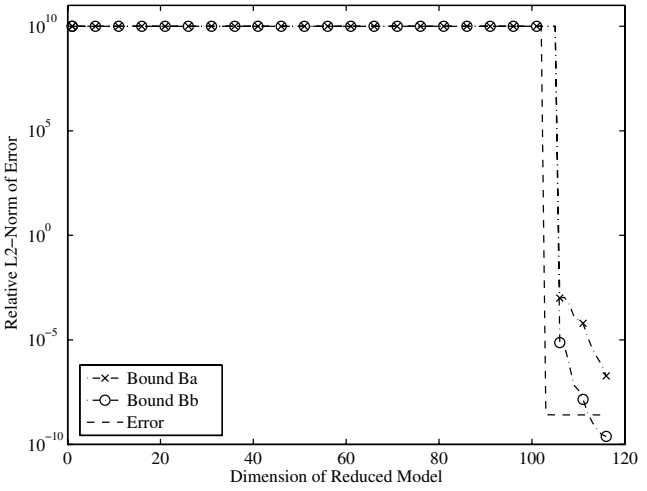

Fig. 8 Integrated error bound $I_{2,\mathrm{rel}}$ vs model size for Krylov projection method. Low-frequency band example BCSST24. The force vector is $\boldsymbol{f} = \boldsymbol{e}_1$.

the slow convergence in plateaus of the modal condensation approximation, looking only at the approximation from one model to the other in a plateau might let one think that the approximation has converged to the solution. The bounds allow one to quantify the quality of the approximation without computing the exact error. Results are similar for $\boldsymbol{f} = \mathbf{a}$. The results for the Ritz condensation and Krylov projection methods in Fig. 7 and 8, respectively, still show that it is better to keep the whole Krylov subspace than it is to extract and keep only the accurate eigenpairs. The history of the iterations for the projection method is presented in Table 4.

Table 4 Low-frequency band example BCSST24; case $\boldsymbol{f} = [1, 0, \ldots, 0]$, history of iterations when using a single Krylov subspace at $\sigma = \lambda_{\mathrm{band}}/2$

Dimension of approximation	N_{miss}	N_{prec}
76	14	40
80	12	45
85	9	57
90	6	60
95	3	63
100	1	63
105	0	73
110	0	76

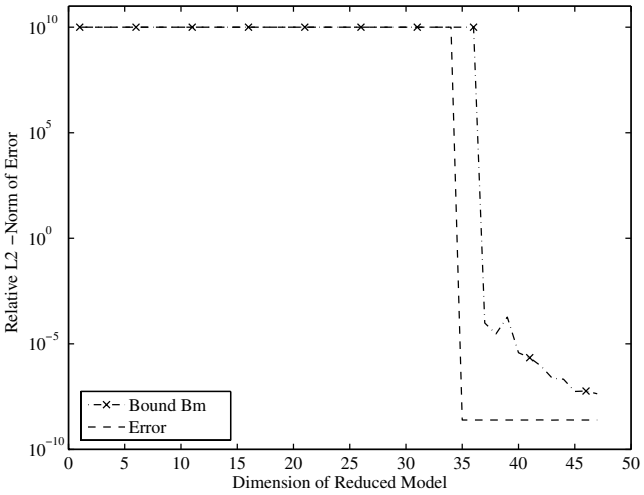

Fig. 9 Integrated error bound $I_{2,\mathrm{rel}}$ vs model size for Krylov projection method. Midfrequency band example BCSST24. The force vector is $f = e_1$.

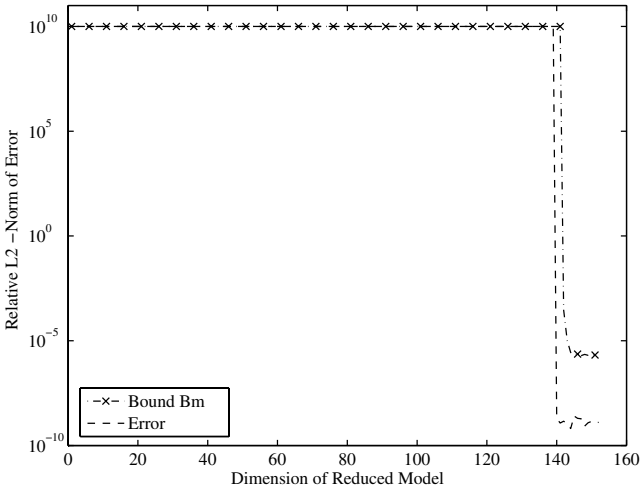

Fig. 10 Integrated error bound $I_{2,\mathrm{rel}}$ vs model size for Krylov projection method. Midfrequency band example BCSST25. The force vector is $f = e_1$.

G. Midfrequency Examples

In this section, results are presented in the midfrequency band for the two largest problems. The Krylov projection method is used and the force vector is equal to $f = e_1$ for each problem. Similar behaviors are seen for the two models in Figs. 9 and 10. In each case, the error is practically (or actually) infinite until a point where the model suddenly and dramatically "converges." Both the exact error and the error bounds exhibit this behavior. In both cases, the number of Krylov vectors necessary for convergence is slightly overestimated by the bounds. In Fig. 9 (respectively, 10), one can see that the model converges at $M = 35$ (respectively, $M = 140$), whereas the error bound predicts convergence at $M = 37$ (respectively, $M = 142$). It can be noted in Tables 5 and 6 that extra Ritz pairs may be present in the band when using Krylov projection methods. The authors experienced in their calculations the general trend that extra Ritz pairs have both large error bounds on their eigenvalues and small magnitude of their modal components, $c^T \tilde{\phi}_m \tilde{\phi}_m^T f$. Two conclusions can be drawn from this observation. First, the superfluous Ritz pairs can be easily identified by sorting the bounds on the eigenvalues. The only confidence intervals to consider are the ones with the smaller bounds. Second, due to the small magnitude of their modal components, the extra Ritz pairs have only a small contribution to the transfer function and they can therefore be removed from the interval of interest without impairing the quality of the approximation. The error introduced thereby is appropriately taken into account in the subsequently computed error bound.

Table 5 Midfrequency band example BCSST24; case $f = [1, 0, \ldots, 0]$; history of iterations when using a single Krylov subspace at $\sigma = (\lambda_{\min} + \lambda_{\max})/2$

Dimension of approximation	N_{miss}	N_{prec}
15	4	3
20	2	7
25	2	10
30	1	11
34	−1	12
35	0	12
38	0	13
39	−1	12
40	0	13
45	0	15

Table 6 Midfrequency band example BCSST25; case $f = [1, 0, \ldots, 0]$; history of iterations when using a single Krylov subspace at $\sigma = (\lambda_{\min} + \lambda_{\max})/2$

Dimension of approximation	N_{miss}	N_{prec}
79	27	30
80	26	29
90	21	31
100	17	38
110	12	39
120	7	44
130	3	53
138	0	62
139	−1	62
145	0	79
146	−1	79
150	0	79

VII. Conclusions

Dynamic condensation methods yield efficient and often accurate approximations of the dynamic response of vibrating systems. Here, error bounds were presented that can be used to assess the accuracy of such approximations of typical undamped systems within a given frequency band of interest. The bounds apply to any Rayleigh–Ritz-based condensation method, including modal condensation, Guyan reduction [9], Wilson et al.'s method [10], component mode synthesis [20], Padé Via Lanczos (PVL) [1,2], forced response condensation [4], and other Krylov and rational Krylov projection methods [5,6].

The performance of the bounds were evaluated in three different mechanical/matrix systems, and with three different condensation methods. In a wide variety of systems and methods tested here, the behavior of the error bounds mimics the behavior of the true error. Both the behavior of the error with frequency and the integrated error as a function of model size were examined. In the examples considered, the bounds not only bound the error, but are sharp enough to accurately estimate the error.

One of the key intended applications of error bounds is the determination of the minimum model size required to accurately capture the dynamic response of a structure. This issue was explored with several different models and several condensation methods. With modal condensation, for example, one observed very slow convergence with model size, indicated by both the true error and the error bounds. Evident are several plateaus in the response at relatively large error. If one were using a heuristic based on computed change in the response with model size, without error bounds, one might be deceived into thinking a reduced model is accurate as soon as the first plateau is reached, regardless of the level of that plateau. One noted dramatically different behavior of the exact error in the examples with Krylov reduction. The error bounds nevertheless mimicked the behavior of the exact error quite closely. The examples

tested here suggest that using the error bound to truncate the model with Krylov methods would result in using only a few more Krylov vectors than absolutely necessary to obtain an accurate result. One concludes that the bound would be useful in forming a termination criterion for iterative condensation methods.

Here, the simplest available error bounds on eigenvalues and eigenvectors were used. Although these were adequate for the examples considered here, more accurate error bounds on the overall response can be obtained by using more accurate error bounds on the eigenvalues and eigenvectors. Among the possibilities are the bounds presented in [15], Chapter 5. The error bounds on the transfer function could also be extended to support cluster bounds on the eigenvalues.

In practical applications, the issue of the cost of evaluating the bounds is critical. The bounds presented here can be updated efficiently and cheaply ([15], Chapter 7) at each step of a Lanczos process or a rational Krylov projection method. Finally, the derivation presented here can serve as a framework to derive other bounds. These may be obtained by using other exact expressions of the error as a starting point ([15], Chapter 6) and following the general procedure outlined herein.

Acknowledgments

This material is based upon work supported by the National Science Foundation under Grants 9978747 and 9984994.

References

[1] Feldmann, P., and Freund, R. W., "Efficient Linear Circuit Analysis by Padé Approximation via the Lanczos Process," *Proceedings of EURO-DAC'94 with EURO-VHDL'94*, Inst. of Electrical and Electronics Engineers, New York, 1995, pp. 170–175.

[2] Gallivan, K., Grimme, E., and Van Dooren, P., "Asymptotic Waveform Evaluation via a Lanczos Method," *Applied Mathematics Letters*, Vol. 7, No. 5, 1994, pp. 75–80. doi:10.1016/0893-9659(94)90077-9

[3] Lanczos, C., "An Iteration Method for the Solution of the Eigenvalue Problem of Linear Differential and Integral Operators," *Journal of Research of the National Bureau of Standards (United States)*, Vol. 45, No. 4, 1950, pp. 255–282.

[4] Lecomte, C., McDaniel, J. G., Barbone, P. E., and Pierce, A. D., "Efficient High-Order Frequency Interpolation of Structural Dynamic Response," *AIAA Journal*, Vol. 41, No. 11, Nov. 2003, pp. 2208–2215.

[5] Grimme, E. J., "Krylov Projection Methods for Model Reduction," Ph. D. Thesis, Dept. of Electrical and Computer Engineering, Univ. of Illinois at Urbana–Champaign, Urbana, IL, May 1997.

[6] Ruhe, A., "Rational Krylov: A Practical Algorithm for Large Sparse Nonsymmetric Matrix Pencils," *SIAM Journal on Scientific Computing*, Vol. 19, No. 5, 1998, pp. 1535–1551. doi:10.1137/S1064827595285597

[7] Padé, M. H., "Sur la Représentation Approchée d'une Fonction par des Fractions Rationnelles," Ph.D. Thesis, Faculté des sciences de Paris, Académie de Paris, Paris, 1982.

[8] Baker, G. A., and Graves-Morris, P. R., *Padé Approximants*, Vol. 59, Encyclopedia of Mathematics and its Applications, 2nd ed., Cambridge Univ. Press, Cambridge, England, U.K., 1996.

[9] Guyan, R. J., "Reduction of Stiffness and Mass Matrices," *AIAA Journal*, Vol. 3, No. 2, 1965, p. 380.

[10] Wilson, E. L., Yuan, M.-W., and Dickens, J. M., "Dynamic Analysis by Direct Superposition of Ritz Vectors," *Earthquake Engineering and Structural Dynamics*, Vol. 10, No. 6, 1982, pp. 813–821. doi:10.1002/eqe.4290100606

[11] Bai, Z., and Ye, Q., "Error Estimation of the Padé Approximation of Transfer Functions via the Lanczos Process," *Electronic Transactions on Numerical Analysis: ETNA*, Vol. 7, 1998, pp. 1–17.

[12] Slone, R., "Removing the Frequency Restriction on Padé via Lanczos with an Error Bound," *Proceedings of the 1998 IEEE International Symposium on Electromagnetic Compatibility*, Vol. 1, Inst. of Electrical and Electronics Engineers, New York, 1998, pp. 202–207.

[13] Skoogh, D., "A Rational Krylov Method for Model Order Reduction," Chalmers Univ. of Technology and Univ. of Göteborg, Dept. of Mathematics, TR 1998-47, Göteborg, Sweden, 1998.

[14] Parlett, B., *Symmetric Eigenvalue Problem*, SIAM Classics in Applied Mathematics Series, Prentice–Hall, Upper Saddle River, NJ, 1998.

[15] Lecomte, C., "Analysis of Condensation Methods for Large Structural Dynamic Systems," Ph.D. Thesis, Boston Univ., Dept. of Aerospace and Mechanical Engineering, Boston, MA, May 2007.

[16] Golub, G. H., and Van Loan, C. F., *Matrix Computations*, 3rd ed., Johns Hopkins Univ. Press, Baltimore, MD, 1996.

[17] Bathe, K.-J., *Finite Element Procedures*, Prentice–Hall, Upper Saddle River, NJ, 1996, Chap. 10.4.

[18] Duff, I. S., Grimes, R. G., and Lewis, J. G., "Users' Guide for the Harwell–Boeing Sparse Matrix Collection (Release 1)," Rutherford Appleton Lab., TR RAL 92-086, Chilton, Oxon, England, U.K., 1992.

[19] Boisvert, R. F., Pozo, R., Remington, K., Barrett, R., and Dongarra, J. J., "Matrix Market: A Web Resource for Test Matrix Collections," *Quality of Numerical Software, Assessment and Enhancement*, edited by R. F. Boisvert, Chapman & Hall, London, 1997, pp. 125–137.

[20] Craig, R. R., Jr., Coupling of Substructures for Dynamic Analysis: An Overview, AIAA 2000-1573, 2000.

J. Wei
Associate Editor